Physica A 391 (2012) 6347–6361

Contents lists available at SciVerse ScienceDirect

Physica A

journal homepage: www.elsevier.com/locate/physa

The fractal energy measurement and the singularity energy spectrum analysis

Gang Xiong [a,b,*], Shuning Zhang [a], Xiaoniu Yang [b]

[a] Electronic Engineering Department, Nanjing University of Science and Technology, Nanjing, 210094, China

[b] NO.36 Research Institute of CETC, National Laboratory of Information Control Technology for Communication System, Jiaxing, 314001, China

ARTICLE INFO

Article history:
Received 18 February 2012
Received in revised form 8 July 2012
Available online 27 July 2012

Keywords:
Fractal energy measurement
Singularity energy spectrum
Fractal sub-band signal
Stochastic multifractal Spectrum
Hausdorff measure

ABSTRACT

The singularity exponent (SE) is the characteristic parameter of fractal and multifractal signals. Based on SE, the fractal dimension reflecting the global self-similar character, the instantaneous SE reflecting the local self-similar character, the multifractal spectrum (MFS) reflecting the distribution of SE, and the time-varying MFS reflecting pointwise multifractal spectrum were proposed. However, all the studies were based on the depiction of spatial or differentiability characters of fractal signals. Taking the SE as the independent dimension, this paper investigates the fractal energy measurement (FEM) and the singularity energy spectrum (SES) theory. Firstly, we study the energy measurement and the energy spectrum of a fractal signal in the singularity domain, propose the conception of FEM and SES of multifractal signals, and investigate the Hausdorff measure and the local direction angle of the fractal energy element. Then, we prove the compatibility between FEM and traditional energy, and point out that SES can be measured in the fractal space. Finally, we study the algorithm of SES under the condition of a continuous signal and a discrete signal, and give the approximation algorithm of the latter, and the estimations of FEM and SES of the Gaussian white noise, Fractal Brownian motion and the multifractal Brownian motion show the theoretical significance and application value of FEM and SES.

1. Introduction

The idea of describing natural phenomena by statistical scaling analysis, the self-similarity and self-affine character, has a long history. Indeed, many researches have been carried out on this topic. In the 1960s, fractal master Mandelbrot published his landmark book, and then, the conception and the status of fractal geometry were set up progressively. Subsequently, the study on the Hausdorff measurement and dimension, singularity exponent, multifractal spectrum as well as various definitions of fractal dimension and its application plays the dominant role in the fractal theory [1–4].

The advantage of fractal theory is aimed primarily at the seemingly irregular and not smooth singularity debris, which exists widely in the real world and cannot be solved using traditional measures and set theory. The fractal theory using temporal and spatial statistical scaling law and the power-law characteristic can reveal that complex dynamic systems widely

* Corresponding author at: Electronic Engineering Department, Nanjing University of Science and Technology, Nanjing, 210094, China. Tel.: +86 13761230701; fax: +86 02584315843.
E-mail addresses: honey_xiong@163.com, pdxiong@gmail.com (G. Xiong), shuningzhang0704@163.com (S. Zhang).

0378-4371/$ – see front matter
doi:10.1016/j.physa.2012.07.056

exists in the real world. The applications of fractal theory in signal processing developed fractal signal processing. Researches show that fractals are fit for signal analysis, processing and modeling in the real world, such as electroencephalogram (EEG), electrocardiogram (ECG), as well as turbulent flows, lightning strikes, DNA sequences, and geographical objects which represent some of many natural phenomena and are difficult to be characterized using traditional signal processing theory [4–6]. Therefore, the fractal theory provides a new train of thought for complex system research, non-stable and non-linear signal processing.

Fractal dimension describes the geometry characters of fractal signals, including the measurement of complexity, singularity and irregularity of the signal, whose estimations are the key problem of fractal theory [4]. Stanley and Ostrowsky [7] and Pietronero and Tosatti [4] have been pioneers in the development of this research and studied the fractals in physics [4,7]. In the past decades, various definitions and algorithms of global fractal dimension have been proposed through the history of fractal theory, which included the measure method, the FBM method and the IFS method [5]. Besides the Hausdorff dimension, several global fractal dimensions were brought forward, such as self-similar dimension, box-counting dimension, capacity dimension, padding dimension, Kolmogorov dimension and Lyapunov dimension, but the relationships among those fractal dimensions are still a puzzle, and they are all based on the idea of "the measure under the scale δ" [5].

The multifractal formalism is based on the calculation of two sets of coefficients associated to the signals: the Holder exponent (HE) that quantifies the local regularity of a signal or function and the multifractal spectrum (MFS) that quantifies the multifractality of the signal and measurement. The MFS associates each group of data with the same regularity with the Hausdorff dimension of this point set. In this way, it defines a function between the HE and the Hausdorff dimension which is also known as spectrum of singularity [5,6]. The MFS is intimately related with the generalized Hausdorff dimension of strange attractors based on which Grassberger and Procaccia have published studies widely, in the 1980s [5,6,8]. In 1988, Chhabra and co-workers studied the relationship between the MFS and the entropy density of fractal system, and related the Holder exponent with the free energy of a fractal set [9,10]. After that, Arneodo, Bacry and Muzy proposed the wavelet transform modulo maxima (WTMM) method, a statistical method for the estimation of the MFS based on the study of the maxima of the continuous wavelet coefficients of the signal [11–13]. In 1995, Peng and collaborators put forward the detrended fluctuation analysis (DFA) [14], which was proved to adapt the short datasets and has less computational complexity and was successfully applied to the study of sequences of DNA, non-stationary heartbeats time series, human brain electroencephalogram, physiological and economical processes [15–18]. After that, Castro *e* Siva and Moreira introduced the conception of the generalization of the DFA, and subsequently, Kantelhardt et al. proposed the multifractal detrended fluctuation analysis (MFDFA) and its application on the non-stationary time series analysis, which extended the application field for temporary series with multifractal behavior [19,20]. In the past years, Jaffard with Lashermes and Abry have proposed the Wavelet Leaders (WL) method, a new formulation in terms of the local supreme of the wavelet coefficients or Leaders of the signal. The WL is a new methodology for the characterization of Holder exponents and their relationship between Holder regularity and local oscillations [21–25]. Recently, Schumann and Kantelhardt [26] introduced the multifractal centered moving average (MF-CMA) based on the CMA technique [26,27]. In fact, MF-CMA is a special case of multifractal detrending moving average algorithm (MF-DMA) proposed by Gu and Zhou [28] based on DMA proposed by Carbone et al. in 2002 [28]. Jiang and Zhou [29] also concluded that the backward MFDMA performs best, the centered MFDMA performs worst, and the forward MFDMA outperforms the MFDFA [29]. In the calculation of MFS, Arneodo et al. studied the fractal dimensions and multifractal spectrum for Henon attractor [30]. Audit et al. compared the WTMM and DFA, and their performance for LRC analysis is quantitatively analyzed in regards of statistical convergence and finite-size effects [31]. At the same time, the application field of Fractals is developed from the traditional geography structure, meteorological distribution and chemical oscillation to general non-linear and non-stationary signal processing fields.

However, the generality of the above studies is based on the spatial characteristics and the differentiability analysis of the fractal signal or fractal time series, such as the fractal dimension and the singularity exponent, which fail to present the energy distribution of the signal along with the singularity exponent and the hierarchical quality of energy measurement. All previous research such as the Hausdorff measure, Lebesgue measure and multifractal spectrum, only measured the self-spatial size of the fractal subset, but failed to study the energy measurement of the fractal subset instead. To reveal the spatial dynamics character of the fractal system and describe the dynamics of the evolving process of non-stationary and nonlinear system, the conception of fractal energy measurement and singularity energy spectrum are proposed in this paper based on the Hausdorff measure and the singularity analysis.

The rest of this paper is organized as follows. Section 2 is devoted to the theoretic foundation of the fractal energy measurement and the singularity energy spectrum. We distinguish between the fractal subset and the fractal sub-band signal, summarize the algorithm of singularity exponent, and explore the physical meaning, conception, and origins of FEM and SES. Based on the Hausdorff measure, in Section 3, we propose the conceptions and the mathematical expressions of fractal energy measurement(FEM) and singularity energy spectrum(SES) of multifractal signals, study the Hausdorff measure and the local direction angle of the fractal energy element. We also prove the compatibility between the FEM and the traditional Energy. Section 4 studies the algorithm expression of SES under the condition of the continuous signal and the discrete signal, and the approximation algorithm of the latter. In Section 5, we simulate and discuss the FEM and SES of the Gaussian white noise, Fractal Brownian motion and the multifractal Brownian motion. Finally, in Section 6, we provide a conclusion.

2. Theoretical basis and the conception origin

2.1. The fractal sub-band signal

Stochastic fractal signal processing is the combination of fractal theory and signal processing. Divide the fractal set according to the singularity exponent, and call the subsets composed of the little unit with same singularity measurement and power law characteristics as the fractal subsets, denoted as $x(\alpha)$. These fractal subsets from the singularity decomposition construct the compact support of $x(t)$, i.e. $x(t) = \bigcup_\alpha x(\alpha)$. Similarly, in the field of stochastic fractal signal processing, regard the fractal segmentation as the fractal filter, and regard the singularity exponent as the parameter of fractal filter, then $x(\alpha)$ can be considered as the fractal sub-band signal. From the viewpoint of multifractal signal space, suppose F is the multifractal signal/time series, $s \subset 2^F$ (2^F is the power set) is the fractal sub-band signal, α be any measure, and hence (F, s, α) is the fractal signal space. If α is the singularity measure, then $s(\alpha) = \{F_t : \alpha(F_t) = \alpha\}$ is the fractal subset or fractal sub-band signal which satisfies $s(t) = \int_\alpha s(\alpha)\mathrm{d}\alpha$ or $s(t) = \sum_\alpha s(\alpha)$.

2.2. Several definitions of singularity exponent

According to the multifractal theory, set x is any subset with topology dimension d, and μ is a Borel measure on x. Decompose iteratively (x, μ) with α, and after n steps, the cells with the same measure $\mu(\alpha)$ structure the subset $x(n, \alpha)$. If $\lim_{n\to\infty} x(n, \alpha) = x(\alpha)$ is a fractal set, then $x(\alpha)$ is called a fractal subset. Furthermore, define fractal dimension of fractal subset $x(\alpha)$ as $f(\alpha) = \dim[x(\alpha)]$, thus $f(\alpha)$ is the multifractal spectrum of x.

The fractal segmentation differs according to the definition of the singularity exponent. There are three kinds of definitions of singularity exponent. *The first* is the point measurement analysis method. For any point in x, define the singularity exponent (SE) $\alpha(x) = \lim_{r\to 0} \log_2 \mu(B(x, r))/\log_2 r$, where $B(x, r)$ is the closure centered in x with radius r, and μ is the basic measure. Call the subsets composed of the little unit with same singularity measure and power law characteristics as the fractal subsets, denoted as $x(\alpha) := \{x : \alpha(x) = \alpha\}$. This method is the basic definition of the singularity exponent, and also the foundation of singularity and measure analysis of fractal sets. However, it is hard to calculate and not convenient for engineering applications.

The second is the Taylor polynomial approximation method. When satisfying the condition of Taylor series expansion, the singularity exponent can be defined by the polynomial approximation as $h(t) = \liminf_{\varepsilon\to 0} \log_2 \sup_{|u-\tau|<\varepsilon} |v(\tau) - v(u)|/\log_2(2\varepsilon)$, where $v(u)$ is Taylor polynomial expansion. The method fails to estimate the SE if the Taylor expansion condition cannot be satisfied.

The third is the singularity exponent based on the wavelet coefficient. Using the characteristics of adaptive time–frequency window of wavelets, we can realize the tract and location of signal details. The wavelet singularity exponent is defined as $w(t, \tau) = \liminf_{n\to\infty} w_{kn}^{(n)}$, where $w_{kn}^{(n)}(t) := -\log_2 |2^{n/2} W_{n,kn}(t)|/n$, and $W_{n,kn}(t)$ is wavelet coefficient with vanishing moment order $n > h(x)$. Because of the characteristics of vanishing moments, select the wavelet function with higher-order vanishing moment than the differential order, and all the singularity points will be detected. The method is popular and convenient for engineering calculations.

2.3. The physical meaning of singularity energy spectrum

For the fractal subset $x(\alpha)$, the multifractal spectrum $f(\alpha)$ and time varying multifractal spectrum distribution $f(t, \alpha)$ solve the problem of its fractal dimension and time-varying fractal dimension of $x(\alpha)$ [32]. However in this paper we study the energy characteristic of fractal subset $x(\alpha)$ in fractal space of $f(\alpha)$ dimension, which represents energy distribution of fractal signal in singular domain and provides a new conception and perspective for fractal signal processing.

Let us note that the research of FEM and SES is mainly based on three points. *The first* is to consider the logical completeness of the development of fractal theory. Based on studies on multifractal spectrum, short-time multifractal spectrum distribution and the quadratic time-singularity multifractal spectrum distribution, there are even more reasons to believe that the singularity exponent can be considered as an independent dimension in the signal space and can be joined to the research field of fractal theory. It is an inevitable trend in the research of independent dimensions in the signal processing from fractal dimension, instantaneous singularity, time-varying dimension, multifractal spectrum and time varying multifractal spectrum distribution to the FEM and SES analysis.

The second is based on a new thought about the fractal structure, namely the mutual relationship and energy distribution between the fractal dimension (reflecting occupation degree in the geometry space) and SE (reflecting space differentiability) in the process of fractal reconstruction. Thus it is expected to get a new fractal structure through the inverse transform of a given SES and singularity spectrum distribution, which lays a good foundation for the multifractal reconstruction method.

The third is studied as an extensive analysis of the traditional energy conception. Fractal energy measurement (FEM) reflects energy measure of the fractal signal in multifractal signal space, interdependence with the singularity energy spectrum analysis. Compared with the traditional energy analysis, in essence the FEM and SES reflect more clearly the constitute element and mechanism of signal energy, which opens another door for us to study the fractal signal.

3. The fractal energy measurement (FEM) and the singularity energy spectrum (SES)

3.1. The basic measure of fractal subset

The basic measures of Fractal subset $x(\alpha)$ are the Hausdorff measure and the Lebesgue measure. For arbitrary δ-coverage of $x(\alpha)$, if $0 < \text{diam}\, U_i < \delta$, introduce notation

$$H_\delta^r(x(\alpha), \mu(\alpha)) = \inf\left\{\sum_{i=1}^{\infty}(\text{diam}\, U_i)^r : x(\alpha) \subset \bigcup_{i=1}^{\infty} U_i\right\}. \tag{1}$$

According to the definition of the Hausdorff measure, the r-dimension Hausdorff measure about μ is

$$H^r(x(\alpha), \mu(\alpha)) = \lim_{\delta\to 0} H_\delta^r(x(\alpha), \mu(\alpha)). \tag{2}$$

If there exists a critical exponent $f(\alpha)$, it satisfies

$$H^r(x(\alpha), \mu(\alpha)) = \begin{cases} 0 & r > f(\alpha) \\ \infty & r < f(\alpha) \\ A & r = f(\alpha), \end{cases} \tag{3}$$

where A is a limited positive number. Then $f(\alpha)$ is the singularity spectrum in the Hausdorff measure with varying α, which is exactly the Hausdorff dimension of $x(\alpha)$

$$f(\alpha) = \inf\left\{r : \lim_{\delta\to 0}\inf\sum_{i=1}^{\infty}(\text{diam}\, U_i)^r = 0\right\} = \sup\left\{r : \lim_{\delta\to 0}\inf\sum_{i=1}^{\infty}(\text{diam}\, U_i)^r = \infty\right\}. \tag{4}$$

Besides Hausdorff measure, there are Lebesgue measure, point measure and so on, and the application scope and calculation of characteristics of those measures are not identical. The Hausdorff measure and Hausdorff dimension theory indicate that only in the fractal space of $f(\alpha)$ dimension can the fractal subset $x(\alpha)$ be Hausdorff measurable. *Firstly*, the above enlightenment inspires us that in order to maintain a consistent testability, FEM and SES must also be defined and measured in $f(\alpha)$ dimension fractal space in seeking for the energy measurement of $x(\alpha)$. *Secondly*, the Hausdorff measure survey generalized measure of signal space occupied by the fractal signal or subset, while the SES measures signal energy of fractal sub-band signal $x(\alpha)$ accumulated by the Hausdorff measure along with the time, which indicates that the study of Hausdorff measure can be considered as the basis of the study of FEM and SES.

3.2. The FEM and SES

Let X be a set of signal or time series, and $x(t) \in X$, $(0 \le t \le T)$ be the continuous signal. Define $x_\alpha(t) = \{x(t) : \alpha(x(t)) = \alpha\}$ as the fractal sub-band signal or fractal subset of signal $x(t)$, then the time index set corresponding to $x_\alpha(t)$ constitutes the set $t(\alpha) = \{t, \alpha(x(t)) = \alpha\}$, i.e.

$$x_\alpha(t) = \begin{cases} x(t) & t \in t(\alpha) \\ 0, & t \in [0, \mathrm{T}] \setminus t(\alpha) \end{cases} \tag{5}$$

where $\alpha(x(t))$ is the singularity exponent of $x(t)$ at time t. According to the multifractal theory, $x(t)$ is a dense subset supported with compact set $\bigcup_a x_\alpha(t)$. At the same time, $x_{\alpha_1}(t), x_{\alpha_2}(t), x_{\alpha_3}(t), \ldots$ constitute the segmentation of $x(t)$, where $x_{\alpha_i}(t)$ are disjointed mutually, namely $x_{\alpha_i}(t) \bigcap x_{\alpha_j}(t) = \varphi, i \ne j$. All measurable subsets constitute a set system $I = \{x_{\alpha_1}(t), x_{\alpha_2}(t), x_{\alpha_3}(t), \ldots\}$, and I is a topology measurable set. There exists a measurable function $f : I \to \Re^+$, and (X, I, f) constitutes a measurable space.

Compared to traditional energy definition of signals, the energy measure of a fractal sub-band signal or fractal subset is different. Although the fractal dimension of $x(t)$ is greater than one, $x(t)$ is still defined in the one-dimensional plane. According to the traditional definition, the energy of fractal signals is the integral of the modulus square of the fractal signal on the time axis. But in fact, if you take a time cell, the dimension of closed space surrounded by signal and cell Δt is greater than 2, and if the signal is the ideal fractal curve with self-similar structure in infinite levels, then the traditional signal energy definition using the linear approximation method will not work. If the signal has a finite hierarchical structure and scaling interval, in the sense of limitation, linear approximation method will be adopt to calculate FEM and SES. Therefore, when the cell is small enough, we can calculate signal energy of the fractal interval signal in view of 2-dimension plane. However, the fractal time element $x(\mathrm{d}t_f)$ should be derived according to Hausdorff measure of the fractal signal. Assuming $x(t)$, $t \in [a, b]$ is fractal signal with finite time support, by the method of the traditional signal energy definition for reference, draw lessons from, insert a number of points in the interval $[a, b]$ homogeneously to calculate energy measure of $x(t)$, and we have

$$a = t_0 < t_1 < t_2 < \cdots < t_{n-1} < t_n = b, \tag{6}$$

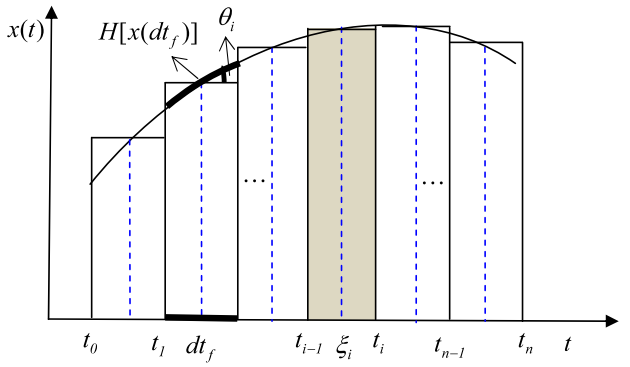

Fig. 1. The fractal time element dt_f, fractal energy element $dW(x(t))$ and the fractal energy measurement $W(x(t))$ obtained from partition of the fractal signal. Divide the interval $[a, b]$ into n segments with interval length Δt_{f_i}. The arc length of $x(dt_f)$ is equal to $H[x(dt_f)]$, and thus $dt_f = H[x(dt_f)]/\sqrt{1 + tg^2\theta_t}$.

which divide the interval $[a, b]$ into n cells $[t_0, t_1], [t_1, t_2], \ldots, [t_{n-1}, t_n]$ with interval length $\Delta t_{f_i} = t_i - t_{i-1}$. Different from the definition of traditional signal energy, in the study of the fractal energy measure, we call Δt_{f_i} the fractal time element. In each time element Δt_{f_i}, some points are selected as $\xi_i \in [t_{i-1}, t_i],\ i = 1, 2, \ldots, n$, with modulus square $|x(\xi_i)|^2$. According to the definition of signal energy, we have

$$W(x(t)) = \sum_{i=1}^{n} |x(\xi_i)|^2 \Delta t_{f_i}. \tag{7}$$

Suppose $\lambda = \max\{\Delta t_{f_i}\}$, when $\lambda \to 0$, the number of divided intervals $n \to \infty$, we have

$$W(x(t)) = \lim_{\lambda \to 0} \sum_{i=1}^{n} |x(\xi_i)|^2 \Delta t_i = \int_a^b |x(t)|^2 dt_f. \tag{8}$$

The fractal time element dt_f can be considered as the projection of fractal signal $x(t)$ on the time axis, which should adopt corresponding measure of fractal signal. In the interval $[t_{i-1}, t_i]$, the length of fractal signal $L\{x(dt_f)\}$ is

$$L\{x(dt_f)\} = dt_f \cdot \sqrt{1 + tg^2\theta_t}, \tag{9}$$

where θ_t is local direction angle of the fractal energy element at $x(\xi_i)$ (discussed later). According to the Hausdorff measure definition of the fractal signal, the length of the fractal signal in the fractal time element dt_f is the Hausdorff measure in the interval dt_f, as showed in Fig. 1, it is

$$H[x(dt_f)] = L\{x(dt_f)\}. \tag{10}$$

Therefore, for the fractal time element, we have

$$dt_f = H[x(dt_f)]/\sqrt{1 + tg^2\theta_t}. \tag{11}$$

The fractal energy element is

$$dW(x(t)) = |x(t)|^2 H[x(dt_f)]/\sqrt{1 + tg^2\theta_t}. \tag{12}$$

Therefore, the fractal energy measure (FEM) can be defined as

$$W(x(t)) = \int [|x(t)|^2/\sqrt{1 + tg^2\theta_t}] H[x(dt_f)]. \tag{13}$$

Then the fractal energy measure of continuous signal can be defined as follows.

Definition 1. For the fractal signal $x(t)$ with $\dim(x(t)) \in [1, 2)$, the fractal energy measurement (FEM) can be defined as

$$W(x(t)) = \int_{-\infty}^{+\infty} [|x(t)|^2/\sqrt{1 + tg^2\theta_t}] dH(x(t)), \tag{14}$$

where $dH(x(t))$ is the differential of the Hausdorff measure of signal $x(t)$. The energy of the fractal signal can be defined as the function of modulus square of the signal, the local orientation angle and the integral of the Hausdorff measure.

For multifractal signals, the calculation of $dH(x(t))$ is related to the singularity exponent. The analysis of fractal time element dt_f and its measure $H[x(dt_f)]$, should distinguish different singular subset $x_\alpha(t)$ with varying singularity exponent, as is the same with fractal energy measure analysis of $x_\alpha(t)$. For arbitrary α, we can calculate the Hausdorff measure element of fractal subset $x_\alpha(t)$, and obtain $dH(\bigcup_\alpha x_\alpha(t))$. So the fractal energy measure should be defined in accordance with the singularity energy spectrum distribution. Hereby we have the following proposition about singularity energy spectrum of a continuous fractal signal.

Proposition 1. *For a multifractal signal, suppose that $x(t)$ can be expressed as a combine of dense subsets $x_\alpha(t)$, which is also known as a fractal sub-band signal or subset, i.e. $x(t) = \bigcup_\alpha x_\alpha(t)$, and then singularity energy spectrum of the fractal signal can be expressed as*

$$\begin{aligned} W[x_\alpha(t)] &= \int_{-\infty}^{+\infty} \left| \frac{|x_\alpha(t)|^2}{\sqrt{1+tg^2\theta_t}}\, dH(x_\alpha(t)) \right. \\ &= \int_{-\infty}^{+\infty} \frac{|x_\alpha(t)|^2}{\sqrt{1+tg^2\theta_t}} H(x_\alpha(dt)), \end{aligned} \tag{15}$$

which can be briefly denoted as $W(\alpha)$, and FEM of multifractal signal can be expressed as

$$\begin{aligned} W(x(t)) &= \int_\alpha W[\alpha] d\alpha \\ &= \int_\alpha \int_{-\infty}^{+\infty} \frac{|x_\alpha(t)|^2}{\sqrt{1+tg^2\theta_i}} dH(x_\alpha(t)) d\alpha. \end{aligned} \tag{16}$$

According to the Hausdorff measure and the definition of fractal energy measure of the fractal signal, the proposition can be proved as follows.

Proof. For multifractal signal, we can calculate singularity exponent $\alpha(t)$ as Section 2.2, and divide the singular sub-band signal or subset $x_\alpha(t)$, so that $x(t) = \bigcup x_\alpha(t)$. For $x_\alpha(t)$, make any δ-coverage $\{U_i\}_{i\in N}$ similar to Hausdorff measure and dimension, so that the coverage meets the $f(\alpha)$ power law and the infimum is bounded, i.e. $\lim_{\delta\to 0} \inf\{\cdot\}$ is a finite value, while the arbitrary two small units have no intersection, i.e. $U_i \bigcap U_j = \phi$, $i \neq j$ and $x_{\alpha i}(t) \bigcap x_{\alpha j}(t) = \phi$, $\alpha_i \neq \alpha_j$. As the Eq. (14), we have:

$$\begin{aligned} W(x(t)) &= W\left(\bigcup_\alpha x_\alpha(t)\right) \\ &= \int_{-\infty}^{+\infty} \frac{\int_\alpha |x_\alpha(t)|^2 d\alpha}{\sqrt{1+tg^2\theta_t}} dH\left(\sum x_\alpha(t)\right) \\ &= \int_{-\infty}^{+\infty} \frac{\sum x_\alpha^2(t) + 2\sum\sum x_{\alpha_i}(t)x_{\alpha_j}(t)}{\sqrt{1+tg^2\theta_t}} dH\left(\sum x_\alpha(t)\right). \end{aligned} \tag{17}$$

Because there is no intersection between $x_{\alpha i}(t)$ and $x_{\alpha j}(t)$, therefore, one has $x_{\alpha_i}(t)x_{\alpha_j}(t) = 0$, $i \neq j$, and

$$\sum\sum x_{\alpha_i}(t)x_{\alpha_j}(t) = 0, \tag{18}$$

$$\sum_\alpha x_\alpha^2(t) dH\left(\sum_\alpha x_\alpha(t)\right) = \sum_\alpha x_\alpha^2(t) dH(x_\alpha(t)). \tag{19}$$

Substituting the above equation into Eq. (17), we have

$$\begin{aligned} W(x(t)) &= \sum_\alpha \int_{-\infty}^{+\infty} \frac{|x_\alpha^2(t)|}{\sqrt{1+tg^2\theta_t}} dH(x_\alpha(t)) \\ &= \int_\alpha \int_{-\infty}^{+\infty} \frac{|x_\alpha(t)|^2}{\sqrt{1+tg^2\theta_i}} dH(x_\alpha(t)) d\alpha \\ &= \int_\alpha W[\alpha] d\alpha. \quad \square \end{aligned} \tag{20}$$

For the mono-fractal, $\alpha = 2 - D$ (D is the fractal dimension), we have

$$W[x(t)] = W[x_\alpha(t)] = \int_{-\infty}^{+\infty} |x(t)|^2 H(x(\mathrm{d}t)). \tag{21}$$

From the above research, we can see that the singularity energy spectrum expresses the energy measure of the multifractal signal in the hierarchy of singularity exponent, which describes the contribution of energy of different singularity exponents, and the distribution of fractal energy in different scales and hierarchy.

3.3. The Hausdorff measure and local orientation angle of fractal element

As Eqs. (14) and (15) indicate, the estimation of Hausdorff measure and local orientation angle of fractal element is crucial when calculating the FEM and SES. In engineering applications, it is very hard to calculate the Hausdorff measure of fractal elements from the mathematical definition of the Hausdorff measure.

When $\{U_i\}_{i\in N}$ are all ε-boxes and the counting of boxes with measure $\mu(\alpha)$ in $[\alpha, \alpha + \mathrm{d}\alpha]$ is $N(\alpha)$. Without loss of generality and allowing for arbitrariness of the covering set, from Eq. (1), we have

$$H_\varepsilon^r(x(\alpha), \mu(\alpha)) = N(\alpha)\varepsilon^r. \tag{22}$$

When $N(\alpha) \sim \varepsilon^{-f(\alpha)}$, $H_\varepsilon^r(x(\alpha), \mu(\alpha))$ is limited, and $f(\alpha) = -\lim_{\varepsilon\to 0} \ln N(\alpha)/\ln\varepsilon$. We can determine the upper bound of $H_\varepsilon^r(x(\alpha), \mu(\alpha))$ based on the two facts. One is the estimating method of multifractal spectrum and partition function based on the wavelet coefficient; the other is the Large Deviation Principle (LDP) and the Legendre transform. From the above relationship, the partition function satisfies [33]

$$S^{(a)}(q) = \sum_{k=0}^{2^n-1} 2^{-nqw_K^{(n)}} = \sum_{|h_K^{(n)}(t)-a|<\varepsilon} 2^{-nqw_K^{(n)}} \geq N^{(n)}(a, \varepsilon)2^{-n(qa+|q|\varepsilon)}, \tag{23}$$

where the partition function $S^{(a)}(q)$ and the mass exponent $\tau(q)$ meet the power law relationship, while $N_t(\alpha)$ and the multifractal spectrum $f(\alpha)$ meet the power law relationship, i.e. $N(\alpha) \sim \varepsilon^{-f(\alpha)}$ and $S^{(a)}(q) \sim 2^{-n\tau(q)}$. Respectively, assume that $N(\alpha) = A(\alpha)2^{-nf(\alpha)}$ and $S^{(a)}(q) = B(q)2^{-n\tau(q)}$, where $A(\alpha)$ is variance about α, and $B(q)$ is variance about q, and we have $A(\alpha) = H_\varepsilon^r(x(\alpha), \mu(\alpha))$ and $B(q) = S^{(a)}(q)2^{n\tau(q)}$. From Eq. (23), we have inequality

$$N^{(n)}(a, \varepsilon) \leq S^{(a)}(q)2^{n(qa+|q|\varepsilon)}. \tag{24}$$

From Eq. (22), we have

$$H_\varepsilon^r(x(\alpha), \mu(\alpha)) = N^{(n)}(\alpha, \varepsilon)\varepsilon^r = N^{(n)}(\alpha, \varepsilon)2^{-nf(a)}, \tag{25}$$

and then

$$H_\varepsilon^r(x(\alpha), \mu(\alpha)) \leq S^{(a)}(q)2^{n(qa-f(a)+|q|\varepsilon)}. \tag{26}$$

Introducing $\tau(q) = qa - f(a)$ and $B(q) = S^{(a)}(q)2^{-n\tau(q)}$ into Eq. (26), we have $A(\alpha) \leq B(q)2^{n|q|\varepsilon}$ and

$$H_\varepsilon^r(x(\alpha), \mu(\alpha)) \leq S^{(a)}(q)2^{-n[\tau(q)-|q|\varepsilon]}. \tag{27}$$

The estimation of the Hausdorff measure is a very complex problem, and up to now the study of the Hausdorff measure still remains in some simple fractal set. This section sets up a bridge between the estimation of the Hausdorff measure and the partition function $S^{(a)}(q)$ through inequality relations of $S^{(a)}(q)$ and $N^{(n)}(a, \varepsilon)$; therefore, the estimation of SES is transformed into the analytical expression about the partition function based on wavelets, multifractal spectrum, weighting factor and the wavelet scale.

Furthermore, we will discuss another parameter, the local orientation angle of the fractal element. Call there exists a tangent θ(unit vector) at x in F, where F is a s set and $F \subset R^n$, if the upper convex density [34]

$$\overline{D}^s(F, x) = \overline{\lim_{r\to 0}} \frac{H^s\left(F \bigcap B(x, r)\right)}{(2r)^s} > 0. \tag{28}$$

Furthermore, for each $\phi > 0$

$$\lim_{r\to 0} r^{-s}H^s\left(F \bigcap B(x, r) \setminus S(x, \theta, \phi)\right) = 0, \tag{29}$$

where $B(x, r)$ centered in x with radius r is a closed circular region; $S(x, \theta, \phi)$ is a double vertebra with vertex located at x and built by the 'y's which makes the maximal angle between the line $[x, y]$ and $\pm\theta$ less than ϕ, and ϕ is the vertex of the double vertebra (see Fig. 2).

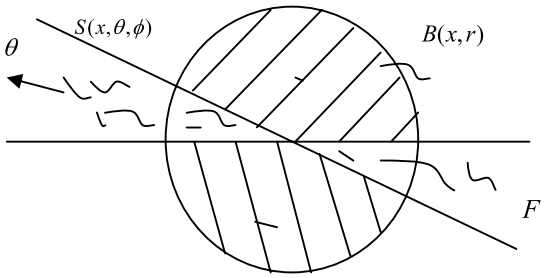

Fig. 2. The local orientation angle of fractal element. If there exists a tangent θ at x in the F, then for little r, the part on $B(x, r) \setminus S(x, \theta, \phi)$ of F can be negligible, which ensures that the effective part of F is close to x in the direction of the tangent θ, while the points of F close to x but outside the double vertebra $S(x, \theta, \phi)$ can be negligible. We call it the local orientation angle of the fractal element.

According to the geometric measure theory and tangent measure theory, when s is an integer, there exists a tangent on set s almost everywhere. For the s set $F \subset R^2$, if $1 < s < 2$, almost all the points on F are not tangent. If $0 < s < 1$, the existence of a tangent on F is inconclusive. The local orientation distribution of set with positive measure is analogous to a tangent line in traditional calculus. For the fractal curve of s set, we will not detail theoretically the local orientation distribution here, but just introduce it into the field of fractal signal processing in view of application.

3.4. The compatibility of definition of SES

For the SES of fractal signal, we have the following compatible propositions.

Proposition 2. *For the fractal signal $x(t)$ with finite time supporting, the definition of fractal energy measure in Eq. (14) is compatible with the traditional energy expression, i.e.,*

$$W(x(t)) = \int_{-\infty}^{+\infty} [|x(t)|^2/\sqrt{1+tg^2\theta_t}]\mathrm{d}H(x(t)) = \int_{-\infty}^{+\infty} |x(t)|^2\mathrm{d}t, \tag{30}$$

where θ_t and $H(\cdot)$ have the same meaning as Eqs. (9) and (14).

Proof. Due to its fractal dimension equal to one, the traditional random signal can be considered as the mono-fractal signal. At the same time, $H(x(\mathrm{d}t))$ is the Hausdorff measure of random signal corresponds to the time element, and then

$$H(x(\mathrm{d}t)) = \lim_{\delta\to 0}\inf\left\{\sum_{i=1}^{\infty}(\mathrm{diam}\, U_i)^r : x(\mathrm{d}t) \subset \bigcup_{i=1}^{\infty} U_i\right\} = L(x(\mathrm{d}t)). \tag{31}$$

$L(x(\mathrm{d}t))$ is the arc length of $x(\mathrm{d}t)$, which satisfies the following equation with tangent angle as

$$L(x(\mathrm{d}t)) = \mathrm{d}t \cdot \sqrt{1+tg^2\theta_t}. \tag{32}$$

According to above analysis and the definition of FEM of fractal signal, we have

$$\begin{aligned} W(x(t)) &= \int_{\alpha}\int_{-\infty}^{+\infty} \frac{|x(t)|^2}{\sqrt{1+tg^2\theta_t}}\mathrm{d}H(x_\alpha(t))\mathrm{d}\alpha = \int_{-\infty}^{+\infty} \frac{|x(t)|^2}{\sqrt{1+tg^2\theta_t}}H(x(\mathrm{d}t)) \\ &= \int_{-\infty}^{+\infty} \frac{|x(t)|^2}{\sqrt{1+tg^2\theta_t}}\mathrm{d}t \cdot \sqrt{1+tg^2\theta_t} = \int_{-\infty}^{+\infty} |x(t)|^2\mathrm{d}t. \quad \square \end{aligned} \tag{33}$$

4. The algorithm analysis of SES

Firstly, we will study the approximation algorithm of SES of a continuous signal. Suppose there exists the bounded function $x = f(t)$ defined on $t \in [0, T]$ with $\dim f(t) \in [1, 2)$. x is the multifractal signal, i.e. $\exists t_1, t_2 \in [0, T]$, s.t. $\alpha(t_1) \neq \alpha(t_2)$, where $\alpha(t)$ is the singularity exponent at t. There exists a fractal subset $x_\alpha(t) = \{(t, f(t)), \alpha(t) = \alpha\}$, which satisfies $\dim[x_\alpha(t)] = f(\alpha)$, and $f(\alpha)$ is the multifractal spectrum. Thus $x_\alpha(t)$s construct the support of $x(t)$, i.e. $x(t) = \bigcup_\alpha x_\alpha(t)$, where $x_\alpha(t)$ is a point set with fractal characteristics.

According to multifractal spectrum theory, $\max(f(\alpha)) = 1$ so except for $\alpha = \arg_\alpha[\max(f(\alpha))]$ all the fractal subsets $x_\alpha(t)$ are sparse and non-continuum. According to the theory of functions of a real variable, $x_\alpha(t)$ is a countable set.

For any α_0, given a small interval $A_0(\delta) = [\alpha_0 - \delta, \alpha_0 + \delta]$, denote $A_0 = \lim_{\delta\to 0} A_0(\delta)$, and correspondingly we have $x_{\alpha_0}(t, \delta) = \{(t, f(t)), \alpha(t) \in A_0(\delta)\}$. Define $x_{\alpha_0}(t) = \lim_{\delta\to 0} x_{\alpha_0}(t, \delta) = \{(t, f(t)), \alpha(t) \in A_0\}$, and $x_{\alpha_0}(t)$ is no longer a countable set but a continuum, so

$$W(\alpha) = \int_{-\infty}^{+\infty} \frac{|x(t)|^2}{\sqrt{1 + tg^2\theta_i}} H(x_\alpha(\mathrm{d}t)) = \lim_{\delta\to 0} \int_{-\infty}^{+\infty} \frac{|x_\alpha(t, \delta)|^2}{\sqrt{1 + tg^2\theta_i}} H(x_\alpha(\mathrm{d}t)). \tag{34}$$

Secondly, for the algorithm of SES of discrete signals, the estimation of the fractal energy spectrum distributions can be modeled as that of the traditional discrete signal. The modulus square of the sampling points can be defined as the discrete signal energy. For the discrete fractal signal $x(n)$, $0 \le n \le N - 1$, calculate the singularity exponent $\alpha(n)$ of discrete points, according to the singularity index, and partition singular subset $x_\alpha(n) = \{(n, x_\alpha(n))\}$. Thus the fractal energy of fractal subset is obtained as

$$W(\alpha) = \sum_n \|x_\alpha(n)\|^2 . \tag{35}$$

To obtain the uniform sample of α, we will study the approximation algorithm of SES of discrete signals. Firstly, calculate the singularity exponent $\alpha(n)$ of discrete points, assume $\alpha(n) \in [\alpha_{\min}, \alpha_{\max}]$, divide the singularity exponent in fixed steps, and obtain singularity exponent vector $\alpha(m) = [\alpha_{\min} = \alpha_0, \alpha_1, \ldots, \alpha_{M-2}, \alpha_{M-1} = \alpha_{\max}]$. For $\alpha(m)$, $0 \le m \le M - 1$, assume $\alpha(m) \le \alpha(n) < \alpha(m + 1)$, define the discrete fractal sub-band signal

$$x_{\alpha_m}(n) = \{(n, x(n))\}, \quad \alpha(n) \in [\alpha(m), a(m + 1)]. \tag{36}$$

Therefore, the SES of a discrete signal can be calculated as

$$W(\alpha_m) = \sum_n \left\|x_{\alpha_m}(n)\right\|^2 . \tag{37}$$

5. The simulation analysis and discussion

To validate the singularity energy spectrum and the fractal energy measure, three kinds of signals are selected for experiment, ① Gaussian white noise (GWN, the non-fractal signal) generated from Matlab7.11; ② Fractal Brownian Motion (FBM, the mono-fractal signal) with singularity $H = 0.4$ generated from; ③ Multifractal Brownian Motion (mFBM, the multifractal signal). For further studies of mFBM, we chose the linear varying mFBM with singularity $H(t) = 0.1 + 0.8t$ and the nonlinear mFBM with $H = 0.5 + 0.3\sin(4\pi t)$ for details. The FBM and mFBM signal was generated from the software envelope "fraclab.2.0.5" in Matlab7.11. The computations have been performed with 10 000 realizations of length $N = 2^{16}$ of GWN, FBM and mFBM to address the statistical convergence and eliminate the finite-size effects of numerical computations.

For the above signals, we simulate the singularity energy spectrum (SES) using the approximation algorithm as defined in Eqs. (35) and (37) in Section 4 and the singular subsets from the singularity decomposition and the fractal sub-band signal of GWN, FBM and mFBM. We compare the theoretical expectation to the numerical experiment with 10 000 realizations of length $N = 2^8, 2^{10}, 2^{13}, 2^{16}$ of GWN, FBM and mFBM. Moreover, we simulate the pointwise singularity exponent (PSE) based on the generalized quadratic variations(GQV) [35] for a 1D signal and multifractal spectrum (MFS) based on the WTMM method of the above signals (also with 10 000 realizations) as a reference to analyze the characteristic of SES and the FEM. Through the simulation of fractal subsets, we study the existence of fractal subset and the divergence of the fractal subsets or signal of three kinds of signals, and discuss the characteristics of SES of the GWN, FMB, linear mFBM and the non-linear mFBM, and their relationship with the MFS and the PSE.

In the following figures, the red dashed lines and red circles correspond to the theoretical exception for PSE, MFS and SES, and the blue lines with different symbols (including •, ◊, □ and ☆) indicate the numerical computation with 10 000 realizations of length $N = 2^8, 2^{10}, 2^{13}, 2^{16}$. Fig. 3 shows the numerical computation of PSE, MFS and SES of GWN. Fig. 3(a) is the GWN with $\sigma^2 = 1$ and length $N = 2^{16}$, and Fig. 3(b) shows the PSE of GWN, which varies in the $[-0.02, 0.04]$, and indicates that the GWN is singular almost everywhere. Fig. 3(c) is the MFS and Fig. 3(d) is the SES of GWN according to the PSE and MFS of GWN, which indicates that the energy of GWN converges and assembles inside the small singular range. Theoretically, PSE of GWN is identically equal to zero and the MFS and SES of GWN exist only at $\alpha = 0$. However, the oscillating of PSE and expansion of MFS and SES were caused by the calculating error. Fig. 4 shows the numerical computation of PSE, MFS and SES of FBM. Fig. 4(a) is the FBM signal with $H = 0.4$ and length $N = 2^{16}$, and Fig. 4(b) shows the PSE of FBM, where the dotted line is the theoretical expectation. The numerical computation of PSE varies in $[0.38, 0.42]$ around the theoretical expectation. Fig. 4(c) is the MFS and Fig. 4(d) is the SES of FBM, which indicate that the energy of FBM converges and assembles around the given singularity exponent, and ideally, the SES of FBM is located at $H = 0.4$, and $W(0.4)$ is the fractal energy measure $W(x)$ of FBM as to the Proposition 1. If we change the Holder exponent, the SES of FBM will move along the singular axis.

We show the numerical computation of PSE, MFS and SES of linear mFBM with Holder exponent $H(t) = 0.1 + 0.8t$ in Fig. 5. Fig. 5(a) is the linear mFBM signal, and Fig. 5(b) shows the PSE of linear mFBM, and the PSE varies as the linear function $H(t)$, which indicates that the linear mFBM has linear varying singularity characteristic. The solid lines are the calculating

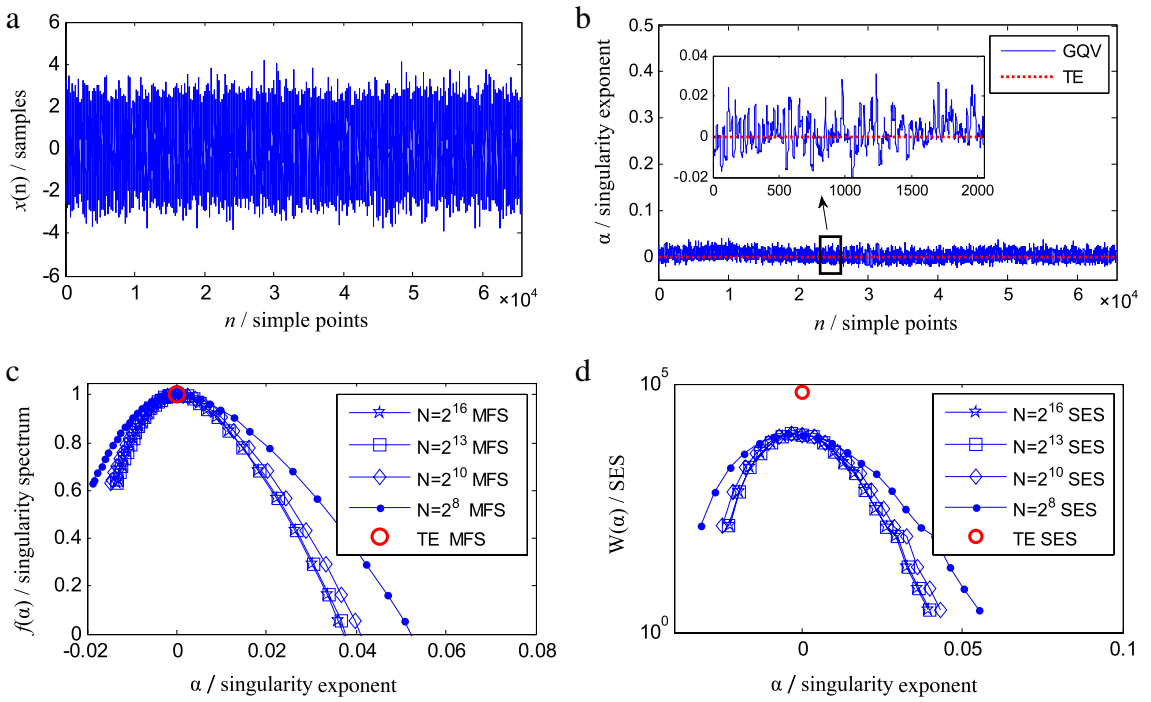

Fig. 3. The numerical computation of fractal characteristic of GWN. (a) the GWN signal with $\sigma^2 = 1$ and length $N = 2^{16}$; (b) the pointwise singularity exponent (PSE) of GWN, based on the generalized quadratic variations (GQV) [35], and the red dotted line corresponds to the theoretic expectation (TE); (c) the multifractal spectrum (MFS) of GWN based on WTMM, where red circle is the theoretic expectation (TE), and (d) the singularity energy spectrum (SES) of GWN with 10 000 realizations based on Eqs. (35) and (37). The solid lines with •, ♢, □ and ☆ correspond to numerical computation of length $N = 2^8, 2^{10}, 2^{13}, 2^{16}$ in (b)–(d). (For interpretation of the references to colour in this figure legend, the reader is referred to the web version of this article.)

computation with different lengths of data, and the dotted line is the theoretical expectation. Those small fluctuations in PSE are caused by the calculating errors. Fig. 5(c) is the multifractal spectrum with length $N = 2^8, 2^{10}, 2^{13}, 2^{16}$, which indicates that when $N = 2^8$, the basis of estimation of MFS is large corresponding to the part of moment $q < 0$, the estimation of $N = 2^{16}$ is close to the theoretical expectation, and the estimation of linear mFBM based on WTMM is statistical convergence. Fig. 5(d) is the SES of linear mFBM, which indicates that the energy of linear mFBM distributes along with singular axis in [0.1, 0.9]. The maxima of SES located in $\alpha_{\max}$ indicates that sub-band signal $x_{\alpha_{\max}}(t)$ is measurable and the fractal energy measure of $x_{\alpha_{\max}}(t)$ is $W(\alpha_{\max})$ in the $f(\alpha_{\max})$ fractal space.

There are several singularity spectrum algorithms currently, including MF-DMA, MF-CMA, Wavelet leader (WL), MF-DFA, WTMM and MFS based on box-dimension. Zhou proposed the MF-DMA and concluded that MFDMA is superior to MFDFA for multifractal analysis [36,37]. Oswiecimka et al. compared WTMM and MF-DFA and concluded that MF-DFA is at least equivalent to WTMM [38]. In Figs. 3–6(c), we use WTMM to calculate the singularity spectrum to explain in auxiliary the physical meaning and the numerical characteristic of their corresponding FEM and SES, because our study indicates that SES is defined in the fractal space with $f(\alpha)$ dimension and the singularity signal subset $x_\alpha(t)$ is measurable with the Hausdorff measure $H_{f(\alpha)}(x_\alpha(t))$ and singularity energy spectrum $w(\alpha)$. It is worth mentioning that the use of MF-DMA in SES analysis is hopeful of further discovering feather of the singularity energy distribution.

In addition, from the Figs. 3–6(c), we can see that the estimations are more accurate when N is larger, and the numerical results indicate that the SES and MFS converge statistically. Furthermore, from the numerical results in Figs. 3(c), (d), 4(c), (d), we can see that the curves of singularity spectrum and SES are artificial multifractality for mono-fractal time series. This is actually a finite-size effect and we can refer to Refs. [36,37], which provide detailed discussions on this topic.

Fig. 6 shows the numerical computation of PSE, MFS and SES of nonlinear mFBM with Holder exponent $H = 0.5 + 0.3\sin(4\pi t)$. Fig. 6(a) is the nonlinear mFBM signal, and Fig. 6(b) shows the PSE of nonlinear mFBM, and the PSE varies as the nonlinear function $H(t) = 0.5+0.3\sin(4\pi t)$, with small fluctuation in PSE, which indicates that the nonlinear mFBM has nonlinear varying singularity characteristic as $H(t)$. Fig. 6(c) is the multifractal spectrum with length $N = 2^8, 2^{10}, 2^{13}, 2^{16}$, which indicates that when $N = 2^8$, the basis of estimation of MFS is large corresponding to the part of moment $q < 0$, the estimation of $N = 2^{16}$ is close to the theoretical expectation, and the estimation of linear mFBM based on WTMM is statistical convergence. Fig. 6(d) is the SES of nonlinear mFBM, which indicates that the energy of nonlinear mFBM distributes along with singular axis in [0.2, 0.8]. For given α, we can get the sub-band signal $x_\alpha(t)$, which is measurable in the $f(\alpha)$ dimension space and the fractal energy measure of $x_\alpha(t)$ is $W(\alpha)$.

Figs. 7–10 show The singular subsets from the singularity decomposition and the fractal sub-band signal of GWN, FBM, linear and non-linear mFBM signal respectively. Numerical computation indicates that the singularity decomposition divides

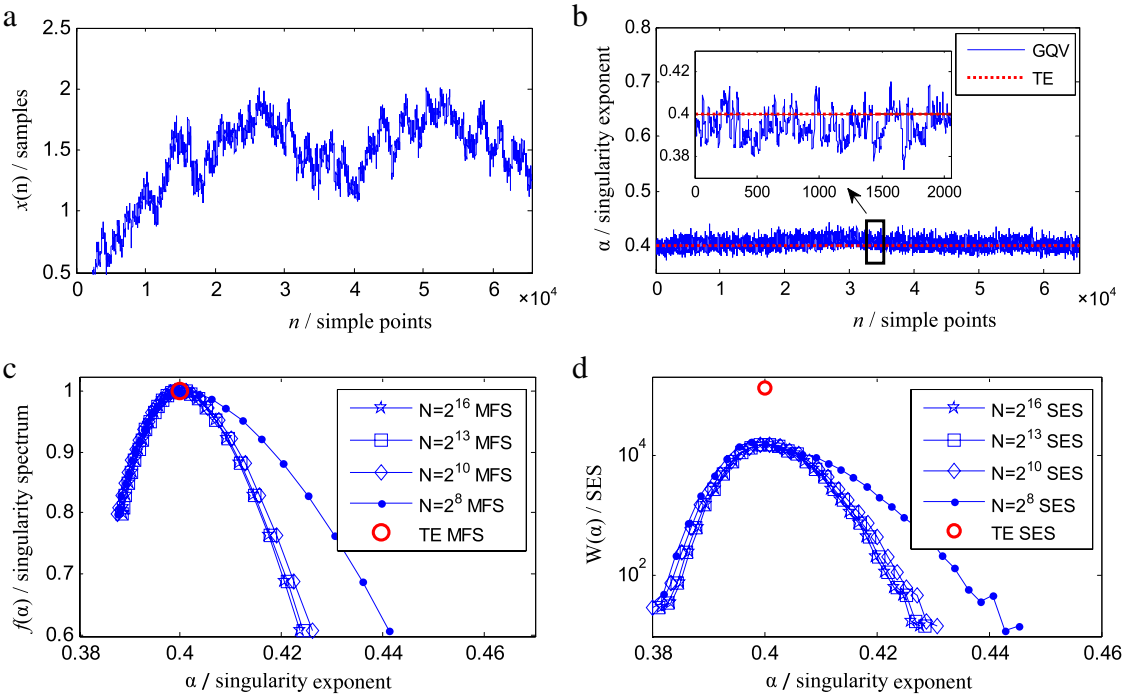

Fig. 4. The numerical computation of fractal characteristic of FBM with $H = 0.4$, where various symbols (•, ◊, □ and ☆) have the same meaning as Fig. 3. (a) the FBM signal with length $N = 2^{16}$; (b) the pointwise singularity exponent (PSE) of FBM, based on the generalized quadratic variations (GQV) [35], and the red dotted line corresponds to the theoretic expectation (TE); (c) the multifractal spectrum (MFS) of FBM based on WTMM, where the red circle is the theoretic expectation (TE), and (d) the singularity energy spectrum (SES) of Fig. 4(a) based on Eqs. (35) and (37). (For interpretation of the references to colour in this figure legend, the reader is referred to the web version of this article.)

the signal with singularity exponent and obtains the fractal sub-band signal, thus the SES is the energy measure of the fractal sub-band signal. For GWN, the fractal sub-band signal is a uniform distribution in the time axis and converges in the given interval of the singular axis, which is consistent with the singularity characteristic of GWN. For FBM, ideally, there only exists a fractal subset with $H = 0.4$. As to the error of numerical calculation, the singularity point is replaced by a small singularity interval. For linear mFBM, the fractal sub-band signal $x_\alpha(t)$ possesses the linear character just as PSE $H(t)$. For example, the $x_{\alpha_0}(t)$ focuses on the time $t_0 = (\alpha_0 - 0.1)/0.8$, and the energy of fractal subset at α_0 originated from the time t_0. For non-linear mFBM, as the PSE varies as $H(t) = 0.5 + 0.3\sin(4\pi t)$, the fractal sub-band signal $x_{\alpha_0}(t)$ includes the points at $t_0 = \arcsin[(\alpha_0 - 0.5)/0.3]/4\pi$. In Figs. 7–10, we can obtain the singularity windows of GWN, FBM and mFBM signal, where the singular subsets from the singularity decomposition are embodied. Furthermore, a time-domain projection window and a singularity-domain projection window exist as shown in Fig. 10. By the time-domain projection and the singularity-domain projection of $x_\alpha(t)$, one can get the fractal signal and the PSE $H(t)$ of fractal signal. From the experiment result of $x_\alpha(t)$, we can see that the singularity decomposition of fractal signal represents the dynamic evolving process and indicates the spatial dynamics character of the system.

Besides, there are three viewpoints worthy of attention. *Firstly*, the calculating deviation of pointwise singularity exponent causes that the simulation of MFS, fractal sub-band signal and the SES are not so ideal. For example, the fluctuation of PSE of FBM leads to the expansion of MFS and SES instead of a single point ideally, which happens to the GWN and mFBM in the same way. So a high accurate estimation of PSE is needed for MFS, SES and FEM. Secondly, we simulated the SES of the fractal signal based on the approximation algorithm of SES of a discrete signal instead of the continuous algorithm of SES as Eq. (34) because it is hard to estimate the local orientation angle and the Hausdorff measure of fractal time element. It lacks rigorous proof that the Parseval theory about energy conservation holds in the fractal field. In Section 3.3, we studied the upper bound of the Hausdorff measure of the fractal element and the existence of local orientation angle θ_t of the fractal element, but more theoretic works about θ_t and $H(x_\alpha(t))$ remain to be done to obtain the continuous singularity energy spectrum $W(\alpha)$. *Thirdly*, the SES is defined in the fractal space and possesses the singularity characteristic, just like the singularity signal subset $x_\alpha(t)$ in the $f(\alpha)$ dimension space with the Hausdorff measure $H_{f(\alpha)}(x_\alpha(t))$. In the loose sense, based on the projection theorem of fractals, the singularity energy measure is defined in the $f(\alpha) + 1$ dimension space. Furthermore, for the mono-fractal signal, and the dimension of singularity energy measure is $D + 1$ dimension. For that discussion, a more strict proof is needed in future research. *However*, these problems could be solved if we consider studying a high accurate estimation of PSE, and explore the physical meaning and mathematic origination deeply. Further studies will be devoted to the algorithm of high accurate estimation of PSE, the local orientation angle and the Hausdorff measure of the fractal time element.

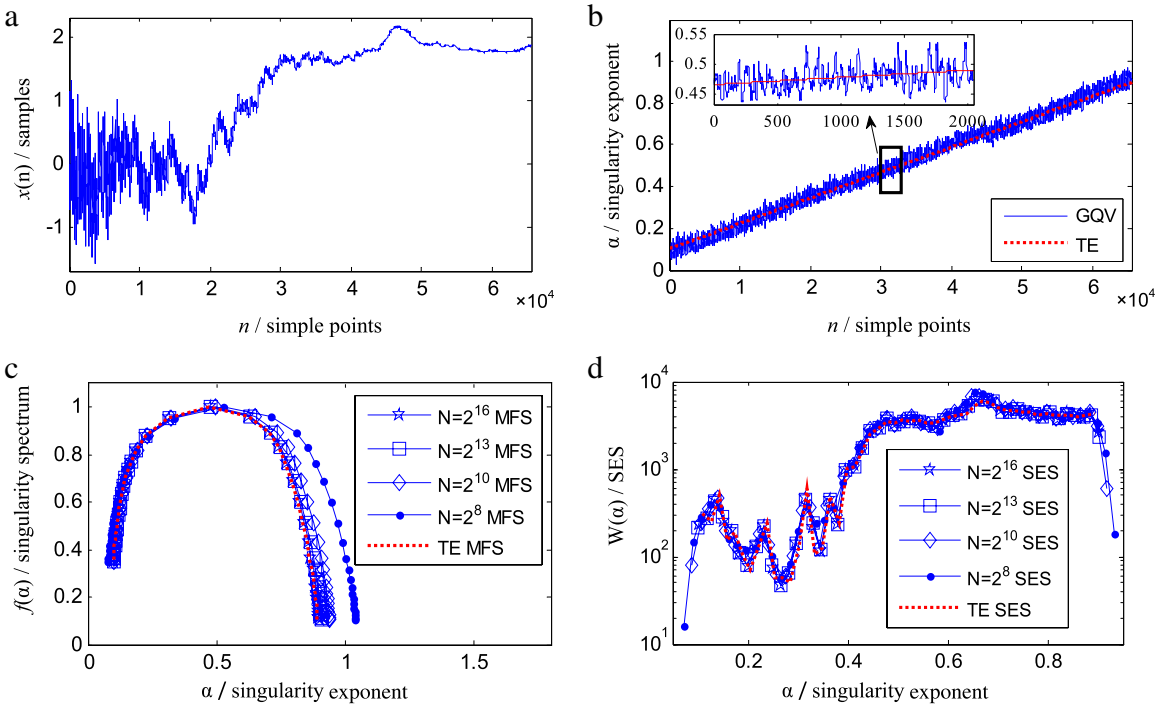

Fig. 5. The numerical computation of fractal characteristic of the linear mFBM with $H = 0.1+0.8t$, where various symbols (•, ◊, □ and ☆) have the same meaning as Fig. 3. (a) the linear mFBM signal with length $N = 2^{16}$; (b) the pointwise singularity exponent (PSE) of linear mFBM, based on the generalized quadratic variations (GQV) [35], and the red dotted line corresponds to the theoretic expectation (TE); (c) the multifractal spectrum (MFS) of linear mFBM based on WTMM, where the red circle is the theoretic expectation (TE), and (d) the singularity energy spectrum (SES) of Fig. 5(a) based on Eqs. (35) and (37). (For interpretation of the references to colour in this figure legend, the reader is referred to the web version of this article.)

It should be noted that this experiment has examined only typical fractal and multifractal signals. For the natural fractal signal in the real world, the validity and feasibility of the SES and FEM remains to be tested. Furthermore, the physical meanings of SES and FEM are still not so distinct. In addition, we should pay attention to application research of SES and FEM on the modulated signal in radar, communication, navigation and measurement and control, which will expand the engineering application of SES and FEM.

6. Conclusion

In this paper, we proposed the conception and the mathematical expression of fractal energy measurement (FEM) and singularity energy spectrum (SES) of multifractal signals, estimated the upper bound of the Hausdorff measure of the fractal element and analyzed the local direction angle of the fractal signal. We also proved the compatibility between the FEM and the traditional energy, and pointed out that SES is measured in the fractal space. We studied the algorithm expression of SES in the condition of the continuous signal and the discrete signal, and gave the approximation algorithm of the latter.

Furthermore, we simulated and calculated the FEM and SES of the Gaussian white noise, fractal Brownian motion and the multi-fractal Brownian motion, and discussed the shortcomings and deficiencies on the calculating precision and the theoretical rigorousness. From the experiment results, we conclude that: (1) the fractal sub-band signals/subsets of GWN, FBM, linear mFBM and non-linear mFBM exist actually based on the singularity decomposition, and they embody the different characteristics of four kinds of signals. For GWN, the fractal subset cluster is only one set with $H = 0$ approximately. For FBM, it is also one set with given H. For mFBM, the fractal subset clusters distribute with different singularity exponents; when $\alpha_{\max} = \max_{\alpha}(f(\alpha))$, the fractal subset $x_{\alpha_{\max}}(t)$ is continuum because $\max(f(\alpha)) = 1$. When the PSE deviates from $\alpha_{\max}$, fractal subsets become sparse sets. (2) The SES represents the energy distribution of the fractal signal based on the fractal energy spectrum along with PSE. The SES of GWN and FBM is one point corresponding to only the fractal sub-band signal in the given Holder exponent, and the FEM of GWN or FBM is in the same way respectively. The SES for mFBM has rich energy distribution about the singularity exponent corresponding to singularity decomposition of the mFBM signal. The experiment showed that the SES is irrelevant with the dimension of the fractal subset, and the SES is not a convex function like the multifractal spectrum function, while the FEM of the mFBM is equal to the integral of the SES along with PSE.

Further studies will concentrate on the high accurate estimation of PSE, the estimation of the local orientation angle and the Hausdorff measure of fractal time element. We will also develop the SES and the FEM to the high dimension signal

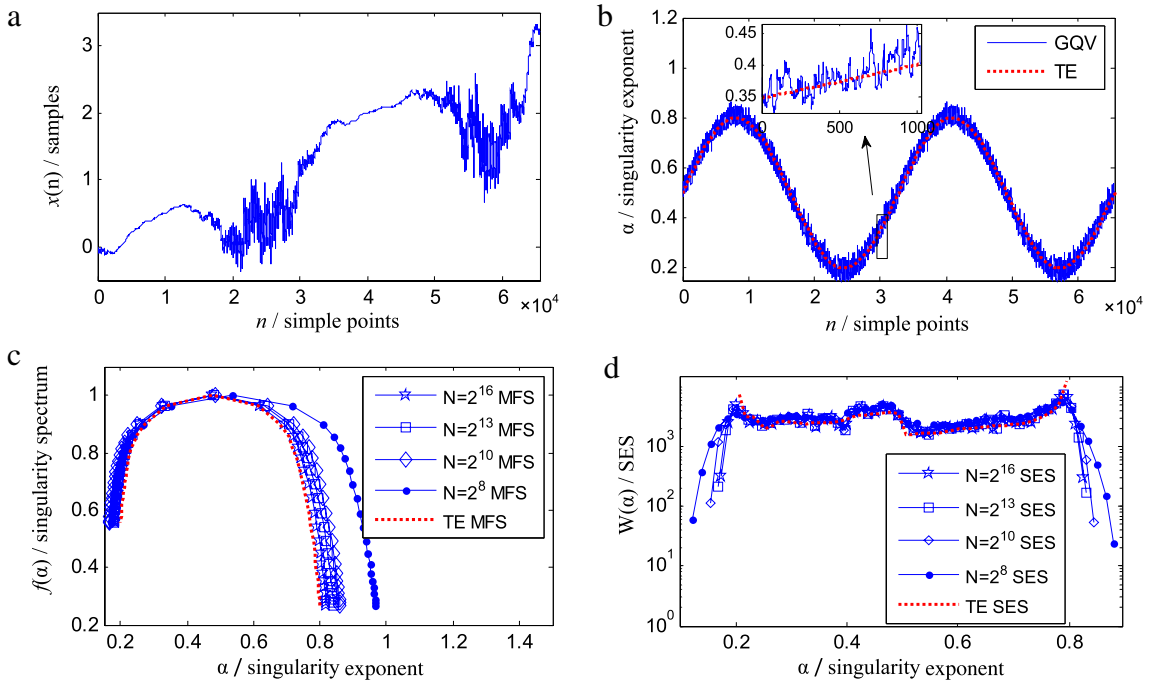

Fig. 6. The numerical computation of fractal characteristic of the nonlinear mFBM with $H = 0.5 + 0.3\sin(4\pi t)$, where various symbols (•, ◊, □ and ☆) have the same meaning as Fig. 3. (a) the nonlinear mFBM signal with length $N = 2^{16}$; (b) the pointwise singularity exponent (PSE) of the nonlinear mFBM based on the generalized quadratic variations (GQV) [35], and the red dotted line corresponds to the theoretic expectation (TE); (c) the multifractal spectrum (MFS) of nonlinear mFBM based on WTMM, where the red circle is the theoretic expectation (TE), and (d) the singularity energy spectrum (SES) of Fig. 6(a) based on Eqs. (35) and (37). (For interpretation of the references to colour in this figure legend, the reader is referred to the web version of this article.)

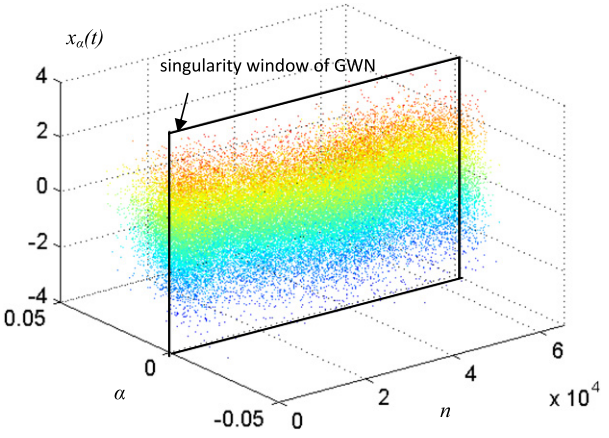

Fig. 7. The singular subsets from the singularity decomposition and the fractal sub-band signal of Gaussian white noise, which is a uniform distribution in the time axis and concentrate on the slice at $H(t) \in [0, 0.06]$.

processing based on the projection theorem of fractals and to the time-varying SES. It is hoped that we can reveal the dynamics evolving process and the spatial dynamics character of fractal nonlinear systems based on the SES and FEM.

Acknowledgments

We would like to thank Prof. H.c. Zhao of Nanjing University of S&T for their support and encouragement towards the research, and Hui Zhao for manuscript revision. We are grateful to the anonymous reviewers for valuable comments and suggestions.

This work was partially supported by National Science Foundation Research of China (NSFC, Grant Number 61171168 and 60702016).

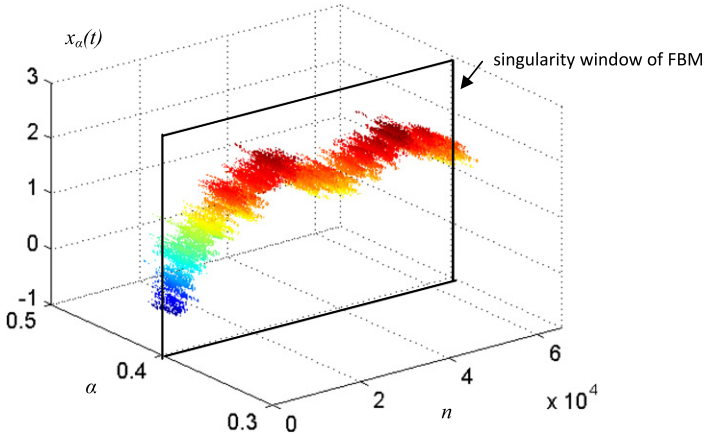

Fig. 8. The singular subsets from the singularity decomposition and the fractal sub-band signal of FBM, which concentrate on the slice at $H(t) = 0.4$. The projection of singularity subsets in the direction of time domain reconstructs the Fractal Brownian Motion signal.

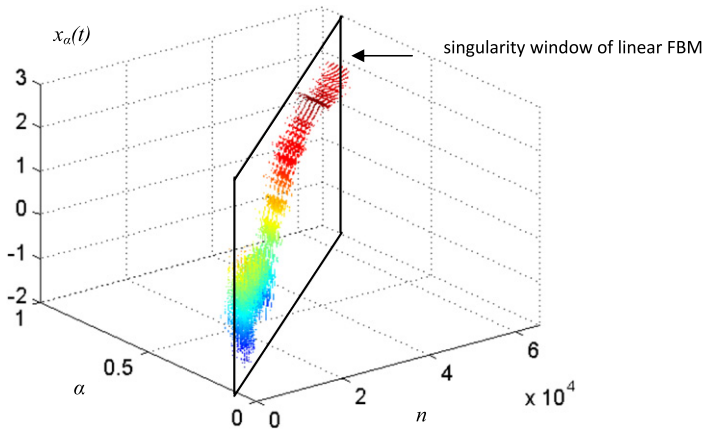

Fig. 9. The singular subsets from the singularity decomposition and the fractal sub-band signal of linear mFBM, which distribute on the time-singularity plane in the law of $t = (\alpha - 0.1)/0.8$. We can reconstruct $x(t)$ according to the singular subsets at $(0.1, 0.1 + 0.8t)$. The projection of singularity subsets in the time-domain or singularity domain can reconstruct the linear mFBM signal according to $H(t) = 0.1 + 0.8t$.

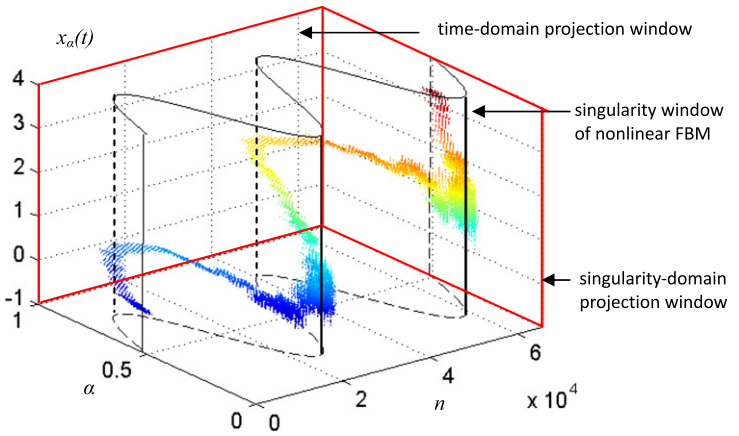

Fig. 10. The singular subsets from the singularity decomposition and the fractal sub-band signal of non-linear mFBM, which distribute on the time-singularity plane in the law of $t = \arcsin[(\alpha - 0.5)/0.3]/4\pi$. We can reconstruct $x(t)$ according to the singular subsets at $(0.2, 0.5 + 0.3\sin(4\pi t))$. The projection of singularity subsets in the direction of the time axis or singular axis reconstructs the non-linear mFBM signal.

References

[1] B.B. Mandelbrot, The Fractal Geometry of Nature, Freeman W.H., San Francisco, 1982, pp. 5–47.
[2] B.B. Mandelbrot, Fractals Form, Chance, and Dimension, Freeman, San Francisco, CA, 1977, pp. 25–35.
[3] B.B. Mandelbrot, Self-affine fractals and fractal dimensions, Phys. Scr. 32 (1985) 257–260.
[4] L. Pietronero, E. Tosatti, Fractals in Physics, North-Holland, Amsterdam, 1986.
[5] P. Grassberger, On the Hausdorff dimension of fractal attractors, J. Stat. Phys. 26 (1981) 173–179.
[6] P. Grassberger, Procaccia measuring the strangeness of strange attractors, Physica D 9 (1983) 189–208.
[7] H.E. Stanley, N. Ostrowsky, On Growth and Form: Fractal and Non-Fractal Patterns in Physics, Nijhoff, Dordrecht, 1985.
[8] P. Grassberger, Estimating the fractal dimensions and entropies of strange attractors, Chaos 1 (1986) 291–311.
[9] A. Chhabra, R. Jensen, Direct determination of the $f(\alpha)$ spectrum, Phys. Rev. Lett. 62 (12) (1989) 1327–1330.
[10] A. Chhabra, C. Maineveau, R. Jensen, K.R. Sreenivasan, Direct determination of the $f(\alpha)$ spectrum and its application on fully develop turbulence, Phys. Rev. A 40 (9) (1989) 5284–5294.
[11] J.F. Muzy, E. Bacry, A. Arneodo, Wavelets and multifractal formalism for singular signals: application to turbulence data, Phys. Rev. Lett. 67 (1991) 3515–3518.
[12] E. Bacry, A. Arneodo, J.F. Muzy, Singularity spectrum of fractal signals from wavelet analysis: exact results, J. Stat. Phys. 70 (1993) 635–674.
[13] A. Arneodo, A. Argoul, J.F. Muzy, Tabard, E. Bacry, Beyond classical multifractal analysis using wavelets: uncovering a multiplicative process hidden in the geometrical complexity of diffusion limited aggregates, Fractals 1 (1995) 629–646.
[14] C.K. Peng, S.V. Buldyrev, A.L. Goldberger, S. Havlin, R.N. Mantegna, M. Simons, H.E. Stanley, Statistical properties of DNA sequences, Physica A 221 (1995) 180–192.
[15] R.B. Govindana, J.D. Wilsona, H. Preil, H. Eswaran, J.Q. Campbell, C.L. Lowery, Detrended fluctuation analysis of short datasets: an application to fetal cardiac data, Physica D 226 (2007) 23–31.
[16] C.-K. Peng, S. Havlin, H.E. Stanley, A.L. Goldberger, Quantification of scaling exponents and crossover phenomena in nonstationary heartbeat time series, Chaos 5 (1995) 82–87.
[17] H.E. Stanley, et al., Anomalous fluctuation in the dynamics of complex systems from DNA and physiology to econophysics, Physica A 224 (1996) 545–552.
[18] C.P. Pan, B. Zheng, Y.Z. Wu, X.W. Tang, Detrended fluctuation analysis of human brain electroencephalogram, Phys. Lett. A 329 (2004) 130–135.
[19] A. Castro e Siva, J.G. Moreira, Roughness exponents to calculate multi/affine fractal exponents, Physica A 235 (1997) 327–333.
[20] J.W. Kantelhardt, S.A. Zschiegner, E. Koscielny-Bunde, S. Havlin, A. Bunde, H.E. Stanley, Multifractal detrended fluctuation analysis of nonstationary time series, Physica A 316 (2002) 87–114.
[21] S. Jaffard, Wavelet techniques in multifractal analysis, fractal geometry and applications: a jubilee of Benoit Mandelbrot, in: M. Lapidus, M. van Frankenhuijsen (Eds.), Proceedings of Symposia in Pure Mathematics Providence, AMS, 2004, pp. 91–151. 72, part 2.
[22] B. Lashermes, S. Jaffard, P. Abry, Wavelet leaders in multifractal analysis, in: Proceedings of IEEE International Conference on Acoustics, Speech, and Signal, IEEE Acoustics, Speech and Signal, vol. 4, 2005, pp. 161–164.
[23] S. Jaffard, Some mathematical results about the multifractal formalism for functions, in: C. Chui, L. Montefusco, L. Puccio (Eds.), Wavelets: Theory, Algorithms, and Applications, Academic Press, 1994, pp. 325–362.
[24] S. Jaffard, Multifractal formalism for functions, parts 1: results valid for all functions and part 2: selfsimilar functions, SIAM J. Math. Anal. 28 (4) (1997) 944–998.
[25] B. Lashermes, S.G. Roux, P. Abry, S. Jaffard, Comprehensive multifractal analysis of turbulent velocity using Wavelet Leaders, Eur. Phys. J. B 61 (2) (2008) 201–205.
[26] Aicko Y. Schumann, Jan W. Kantelhardt, Multifractal moving average analysis and test of multifractal model with tuned correlations, Physica A 390 (2011) 2637–2654.
[27] J. Alvarez-Ramirez, E. Rodriguez, J.C. Echeverria, Detrending fluctuation analysis based on moving average filtering, Physica A 354 (2005) 199–219.
[28] G.-F. Gu, W.-X. Zhou, Detrending moving average algorithm for multifractals, Phys. Rev. E 82 (1 Pt. 1) (2010) 011136. Epub 2010 Jul. 27.
[29] Z.-Q. Jiang, W.-X. Zhou, Multifractal detrending moving average cross-correlation analysis, Phys. Rev. E 84 (1) (2011) 016106.
[30] A. Arneodo, G. Grasseau, Eric J. Kostelich, Fractal dimensions and $f(\alpha)$ spectrum of the Hénon attractor, Phys. Lett. A 124 (1987) 426–432.
[31] B. Audit, E. Bacry, J.F. Muzy, A. Arneodo, Wavelet-based estimators of scaling behavior, IEEE Trans. Inform. Theory 48 (2002) 2938–2954.
[32] G. Xiong, X.n Yang, H.c. Zhao, The short-time multifractal formalism: definition and implement, in: ICIC 2008, CCIS 15, Shanghai, China, 2008. pp. 541–548.
[33] R.H. Riedi, Multifractal processes, Technical Report 99-06, Rice Univ. ECE, June 1999.
[34] Kenneth Falconer, Fractal Geometry: Mathematical Foundations and Applications, John Wiley and Sons Ltd., Wiley, 2003.
[35] A. Ayache, J. Lévy-Véhe, Identification of the pointwise holder exponent of generalized multifractional Brownian motion, Stoch. Proc. Appl. 111 (2004) 119–156.
[36] W.-X. Zhou, The components of empirical multifractality in financial returns, Europhys. Lett. EPL 88 (2) (2009) 28004.
[37] Wei-Xing Zhou, Finite-size effect and the components of multifractality in financial volatility, Chaos Solitons Fractals 45 (2) (2012) 147–155. http://dx.doi.org/10.1016/j.chaos.2011.11.004.
[38] P. Oswiecimka, J. Kwapien, S. Drozdz, Wavelet versus detrended fluctuation analysis of multifractal structures, Phys. Rev. E 74 (2006) 016103.